Heliyon 10 (2024) e36679

Contents lists available at ScienceDirect

Heliyon

journal homepage: www.cell.com/heliyon

Research article

Inhibiting miRNA-146a suppresses mouse gallstone formation by regulating LXR/megalin/cubilin-media cholesterol absorption

Bin Yang, Pingli Cao, Guoqing Bao, Ming Wu, Weihong Chen, Shuangyan Wu, Ding Luo *, Pinduan Bi **

Department of Hepatobiliary Surgery, The First Affiliated Hospital of Kunming Medical University, Kunming, China

ARTICLE INFO

Keywords:
Gallstone
miR-146
Megalin
Cholesterol re-absorption

ABSTRACT

Background: miRNA has been implicated in regulating cholesterol homeostasis, a critical factor in gallstone formation. Here, we focused on elucidating the role of miR-146a in this pathological process.

Methods: C57BL/6 mice were fed with lithogenic diet (LD) and injected with miR-146 antagomir (anta-146) via the tail vein for various weeks. The gallbladders and liver tissues were collected for cholesterol crystal imaging, gallstone mass quantification, and molecular analysis. Levels of cholesterol, bile salt, phospholipids, and metabolic parameters in serum and bile were assessed by ELISA. A 3′ UTR reporter gene assay was used to verify the direct target genes for miR-146. The relative expression of metabolism genes was analyzed by quantitative real-time PCR and immunoblotting.

Results: miR-146a-5p expression was reduced in mice and clinical samples with gallstones. Anta-146 treatment effectively prevented LD-induced gallstone formation in mice without hepatic and cholecystic damage. The mice treated with anta-146 exhibited beneficial alterations in bile cholesterol and bile acids and lipid levels in the blood. A key biliary cholesterol transporter-Megalin was identified as a direct target of miR-146. Anta-146 administration upregulated megalin expression, thereby ameliorating impaired gallbladder cholesterol absorption associated with the LXR-megalin/cubilin pathway.

Conclusion: The data demonstrates that miR-146 modulates gallbladder cholesterol absorption by targeting megalin, and prevents the pathogenesis of cholesterol gallstones.

New & noteworthy text

This study reveals that the administration of anta-146 effectively inhibited the formation of gallstone induced by fedding lithogenic diet in mice, and can elevate LXR-megalin/cubilin pathway to alter gallbladder absorption. Our findings support miRNAs play pivotal role in regulating gallbladder cholesterol absorption in gallstone progression, along with the potential utility of targeting miRNAs as therapeutic options in gallbladder disease.

** Corresponding author. No. 295, Xichang Road, Wuhua District, Kunming, 650000, China.
* Corresponding author. No. 295, Xichang Road, Wuhua District, Kunming, 650000, China.
E-mail addresses: luoding@kmmu.edu.cn (D. Luo), sf581@163.com (P. Bi).

https://doi.org/10.1016/j.heliyon.2024.e36679
Received 4 March 2024; Received in revised form 20 August 2024; Accepted 20 August 2024
Available online 22 August 2024

1. Introduction

Gallstones are a common disease posing a significant threat to human health, leading to complications such as cholecystitis, cholangitis, and pancreatitis, causing great pain to patients [1]. The incidence of gallstones is increasing significantly due to changes in diet and living environment [2]. Numerous risk factors for gallstones, include gender, weight, smoking, exercise, hypertension, hyperlipidemia, diabetes, and coronary heart disease [3]. These lifestyle habits and physical conditions contribute to gallstones formation. The formation of gallstones is complex and closely related to genetic factors [4]. It is widely believed that the basic process of gallstone formation involves the precipitation, nucleation, and growth of bile components [5,6].

Abnormal cholesterol homeostasis has emerged as a significant factor in gallstone formation [4,7]. Recent studies have found differential gene expression in the gallbladder mucosal epithelial cells of humans and guinea pigs between stone and non-stone tissues [8-11]. Dysregulation of these genes controls cholesterol absorption in gallbladder, contributing to cholesterol gallstone development [12]. Corradini et al. [13] reported that cholesterol absorption by the gallbladder significantly decreases in gallstone patients compared to controls. Impaired lipid absorption may serve as an additional factor in cholesterol gallstones formation. Several genes, including ATP-binding cassette transporters G5/G8 (ABCG5/G8), megalin and cubilin, scavenger receptor class B type I (SR-BI), and ABCA1, have been identified in elucidating the mechanisms of cholesterol uptake, intracellular trafficking, and efflux in the gallbladder epithelium [12].

MiRNA (microRNA) is a widely distributed small non-coding RNA of approximately 21-25 nucleotides in size. It mainly binds to the 3′ untranslated region of target mRNA, causing degradation of target mRNA or inhibition of its translation [14]. Studies have shown that miRNAs regulate gene expression at the post-transcriptional level, influencing cell proliferation, differentiation, metabolism, and apoptosis, and are closely related to various metabolic diseases [15,16]. Recent research indicated that miRNAs play a crucial role in cholesterol and lipid metabolism regulation [17,18], contributing to stone disease [19,20]. However, studies on the impact of miRNAs on gallstones are limited, with only miR-223 being extensively studied [21]. Previous high-throughput sequencing identified that miR-146a is differentially expressed between gallbladder tissues of patients with gallstones and normal gallbladder tissues. GO clustering and KEGG pathway analysis showed that miR-146a is mainly enriched in cholesterol transport and absorption metabolism [22]. Studies have shown that miR-146a play an important role in lipid and cholesterol homeostasis regulation [23,24], accounting for gallstone formation. However, the specific role of miR-146a in gallstones development remain unknown, and the mechanism is unclear.

In this study, we established gallstone model in C57BL/6 mice with a high-fat diet and investigated the effect of miR-146a on abnormal cholesterol metabolism and gallstones development. We also focus on miR-146a in modulating the expression of critical factors involved in gallbladder cholesterol absorption.

2. Material and methods

2.1. Gallstone specimens

Thirty specimens of gallstone tissue and twenty-one gallbladder polyps tissue were obtained from fresh surgery specimens. All specimens were immediately fixed in fresh 4 % formaldehyde in the phosphate buffer for 24 h at 4 °C for immunohistochemistry or stored under sterile conditions for RT-qPCR. All the patients from the first Affiliated hospital Hospital of Kunming Medical University from 2020 to 2022, and provided written informed consent for the use of material to research purpose. The study was approved by the Ethics Committee of the First Affiliated Hospital of Kunming Medical University. Human tissue acquisition and its use followed the Institutional Review Board-approved protocol at the Kunming Medical University.

2.2. Animal modeling, gallstone formation and anta-146 treatment

C57BL/6J male mice (8 weeks old, 18–20 g) were purchased from the Animal Laboratory of Kunming Medical University (Kunming, China). The mice were fed with chow diets in plastic cages with environmentally controlled conditions (22 ± 2 °C, a 12 h light cycle) with water for one week. Then, the mice were randomly divided into six groups (n = 10 each group): control group (ctrl), anta-146 group (anta-146), gallstone group (GS), gallstone + anta-NC group (GS + anta-NC), gallstone + anta-146 group (GS + anta-146) and gallstone + ursodeoxycholic acid (UA) group (GS + UA) (for positive control). The GS group was fed lithogenic diets (containing 15 % fat, 1 % cholesterol, and 0.5 % sodium cholate) (Jiangsu Xietong Pharmaceutical Bio-engineering Co., Ltd., Jiangsu, China) for 8 weeks. After 8 weeks of consuming the lithogenic diet, fresh gallbladder bile was taken from mice and evaluated for the presence of microscopic and macroscopic features of gallstone formation, according to criteria described by Zhao et al. [21].

Meanwhile, the normal control group was fed with chow diets. Antagomir-146 used in this study was purchased from Ribo Biotechnology Co., Ltd. After 4 weeks, anta-146 (50 nM, twice/week) or anta-NC (as control, 50 nM, 3 times/week) was injected intravenously via tail vein into mice for 4 weeks. GS + UA groups were given UA (60 mg/kg/d, once every two days) for 4 consecutive weeks. The experiments were conducted following the guidelines of Animal Care and Use Committee of Kunming Medical University (Kunming Medical University, Kunming, China).

2.3. Microscopic examination of cholesterol crystals

Following euthanasia of the mice, gallbladder bile was collected, spread onto glass slides, and examined using a Leica DM6000B polarized microscope to identify cholesterol crystals.

2.4. Bile flow rate measurements

The procedure followed was in accordance with the methods outlined in a previous publication [25]. In brief, male mice underwent a 6-h fasting period with access to water ad libitum. Following ligation of the cystic duct, the common bile duct was cannulated with PE-10 tubing, and hepatic bile was collected for a duration of 30 min to determine the flow rate. Throughout the surgical procedure and bile collection, the mice were anesthetized with isoflurane and maintained at a temperature of 37 °C on a hot plate.

2.5. Hepatic and gallbladder bile, blood, and liver sampling

Mice were anesthetized by intraperitoneal injection of ketamine and xylazine at 80–100 and 5–10 mg/kg, respectively. Following abdominal opening, the cystic duct was ligated, and a common bile duct fistula was created using a polyethylene catheter. Hepatic bile was collected for a duration of 30 min, ensuring the mice remained hydrated, warm, and stable. Subsequently, blood, liver, and gallbladder samples were obtained. The liver samples were promptly frozen at −80 °C. The gallbladder was opened, and bile was extracted. Any gallstones present were separated from the bile using low-speed centrifugation. A portion of the fresh samples underwent biochemical analyses, while the remaining bile was stored at −20 °C until further use.

2.6. Plasma biochemical analyses

Serum alanine aminotransferase (ALT), aspartate aminotransferase (AST), alkaline phosphatase (ALP), total cholesterol (CH), low-density lipoprotein cholesterol (LDL-C), and triglycerides (TG), and high-density lipoprotein cholesterol (HDL-C) were measured by using a Siemens fast automatic biochemical analyzer.

2.7. Hepatic and biliary lipid analyses

The hepatic cholesterol content was determined after lipid extraction. Gallbladder bile cholesterol, phospholipid, and total bile acids (TBA) were examined by an automatic biochemical analyzer UniCelDxC800 (Beckman Coulter, USA). Cholesterol saturation index (CSI), a reliable parameter for biliary saturation with cholesterol, was calculated by mole percent of cholesterol present in bile/maximal amount of cholesterol that would be soluble in bile. The cholesterol saturation of gallbladder bile was determined using critical tables derived from bile samples obtained from mice without crystals and gallstones. Gallbladder cholesterol absorption was measured as described in the previous report [26]. Measurement of Gallbladder Cholesterol Absorption The mice were perfused via the jugular vein with mouse HDL labeled with 5.0 μCi of [14C]cholesterol (NEN Life Science Products, Boston, MA). Exactly 24 h after the perfusion, radioisotopes in gallbladder wall tissue and in gallbladder bile were counted in a liquid scintillation spectrometer and were used for calculating the percent of gallbladder cholesterol absorption: % gallbladder cholesterol absorption = (radioactivities in gallbladder wall tissue ÷ radioactivities in gallbladder wall tissue plus in gallbladder bile) × 100.

2.8. Histological and immunohistochemical assessment of the liver and gallbladder

The liver and gallbladder specimens were prepared and fixed in 4 % neutral-buffered formaldehyde overnight. Subsequently, the specimens were embedded in paraffin and sectioned into 4-μm-thick slices, which were then stained with hematoxylin and eosin (H&E). Following dewaxing, staining, dehydration, clarification, and sealing procedures, the liver and gallbladder specimens were examined under a light microscope (Leica DM6000B Leica Microsystems GmbH, Wetzlar, Germany).

For immunohistochemistry, we use immunohistochemical staining to detect the protein levels of megalin, cubilin, and The liver X receptor (LXR) following the MaxVision™ kit recommendations. The tissue was dewaxed in xylene solution, then rehydrated with gradient ethanol concentrations, and then subjected to antigen retrieval at 100 °C for 15 min with 0.01 mol/lcitric acid (pH = 6.0). Consequently, the slices were incubated in 3%H2O2 to decrease endogenous peroxidase activity and blocked utilizing 10 % goat serum for 30 min to avoid nonspecific antibody binding. Then the anti-megalin antibody (diluted 1: 5000) was added, and the slide was incubated at 4 °C for one night. Then, it was kept at room temperature for 30 min, then rinsed thrice using phosphate-buffered saline (PBS) for 5 min each. The slice was incubated with the secondary antibody for 30 min at room temperature. The staining intensity was scored on the scale from 1 to 4, which included 1) 0 (unstained), 2) 1 (weakly stained), 3) 2(moderately stained), and 4) 3 (strongly stained). Tissues with scores of 2 and 3 were defined as high expression, and those with scores of 0 and 1 were defined as low expression.

2.9. Cell culture and transfection

HEK293T cells were obtained from Kunming wild animal cell bank, the Chinese Academy of Science (China) and maintained in Dulbecco's Modified Eagle's Medium (HyClone, BD), supplemented with 10 % fetal bovine serum plus 1 % penicillin/streptomycin (HyClone). Cells were kept in a 5 % CO2 and 95 % air humidified incubator at 37 °C. miR-146a mimics and negative control (GenePharma, China) were transfected into 293T via Lipofectamine RNAi MAX Transfection Reagent (Thermo Fisher Scientific) according to the manufacturer's instructions.

2.10. Luciferase activity assay

HEK293T cells (5 × 105/well) were cultured in 24-well plates one day before transfection, and then co-transfected with 60 ng The wild type or mutant type of megalin 3′-UTR luciferase reporter plasmids, 20 nM miR-146a mimics or the negative controls by using Lipofectamine 3000 Transfection Reagent (Thermo Fisher Scientific) according to the manufacturer's instructions. Cells were harvested 24 h post-transfection and further subjected to luciferase activity detection by using Luciferase Reporter Assay System (Promega). The results were normalized as the ratio of the reporter luciferase activities to the control firefly luciferase activity.

2.11. Quantitative real-time reverse transcription-polymerase chain reaction (RT-qPCR) assay

Total RNA was extracted from the liver using Trizol reagent (Invitrogen, Carlsbad, CA, USA), followed by reverse transcribed to cDNA using random primers (Invitrogen). Real-time PCR was performed by THUNDERBIRD® qPCR Mix (TOYOBO (SHANGHAI) BIOTECH CO.,LTD., China) with 25 ng template cDNA and 5 mM for each gene-specific primer using the QuantStudio™ 12K Flex system (Thermo Fisher Scientific, Waltham, MA, USA). The PCR conditions and gene-specific primer sequences are detailed in Supplementary Table 1. The quantification of mRNA levels was determined using the mathematical model as described by Pfaffl et al. [27], with mRNA levels of different genes normalized to GAPDH.

2.12. Immunoblotting analysis

Cell membranes were isolated from mouse liver and gallbladder and subsequently prepared for separation on 8 % sodium dodecyl sulfate-polyacrylamide gel electrophoresis (SDS-PAGE). For liver samples, 50 mg of protein was used per sample, while 5 mg was utilized for cell membrane extracts and separated on 8 % SDS-PAGE. Immunoblotting was carried out using antibodies against anti-megalin (19700-1-AP, 1:300 dilution, Proteintech, China), anti-LXR (14351-1-AP, 1:500 dilution, Proteintech, China), and anti-cubilin (sc-518059, 1:300 dilution, Santa Cruz, CA). Antibody binding to protein samples was visualized using enhanced chemiluminescence and measured using the Amersham ImageQuant 800 System (Cytiva, China).

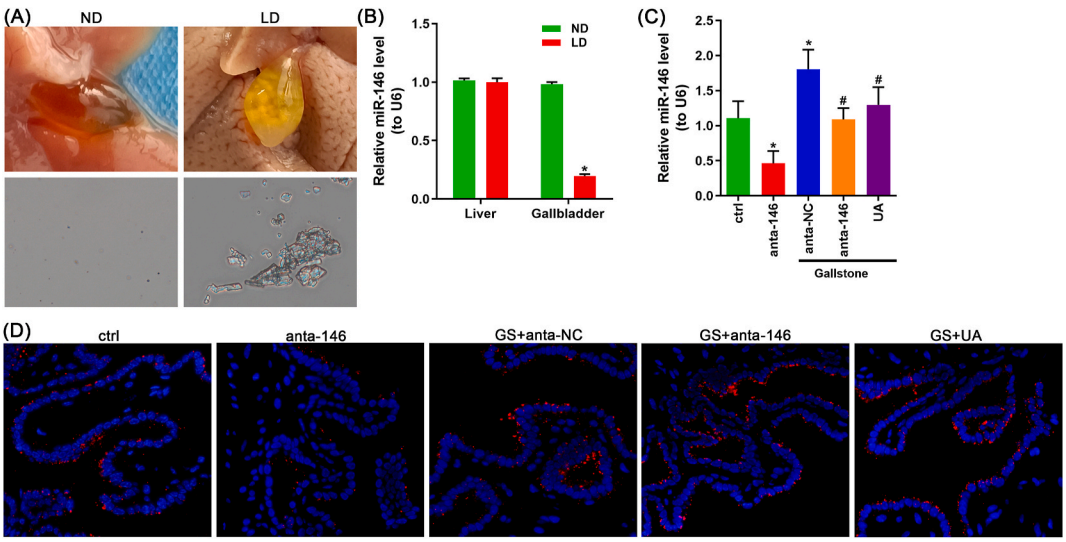

Fig. 1. The expressional alternation of miR-146 in mouse gallbladder and liver during gallstone progression. WT male mice with 8–10 weeks were fed for lithogenic diet (LD) or chow diet for 5 weeks. (A) Representative images showing the gallbladders and cholesterol crystals in bile. Scale bars, 1 mm (gall bladder images) and 250 μm (cholesterol crystal images); (B) RT-qPCR detecting the relative miR-146 expression in gallbladder and liver tissues from chow and LD fed mice with U6 as reference gene (n = 5–6 mice per group). (C) qPCR and (D) FISH hydration detected miR-146 expression in gallbladder sections. Scale bars, 100 μm *p < 0.05 vs. ND or ctrl. UA, ursodeoxycholic acid.

2.13. Fluorescence in situ hybridization (FISH)

FISH was employed to localize miR-146 within tissues. The m-miR-146_FISH Probe Mix was procured from Guangzhou exons biological technology Co., Ltd. (China). After washing the slides with PBS, the cells were fixed with 4 % formaldehyde for 10 min and washed with PBS. FISH was then conducted following the kit protocol. Under light protection, 2.5 μL of 20 μM miRNA FISH Probe Mix stock solution was added to 100 μL of hybridization solution. Each slide received 100 μL of hybridization solution containing the probe and was hybridized overnight at 37 °C, shielded from light. Following staining with DAPI staining solution, the slides were carefully removed from the wells, fixed with sealer, and examined using the Zeiss 510 laser confocal microscope (Zeiss Fluorescent Microsystems, Göttingen, Germany).

2.14. Statistical analysis

Data were expressed as mean ± S.D. The Shapiro-Wilk test was used to verify whether the data were normally distributed. Statistical significance was evaluated by using the Student's t-test or Mann-Whitney *U* test, depending on data distribution. The data were analyzed by a one-way ANOVA followed by a Dunnett's post hoc analysis for multiple comparisons (PRISM 9.0, GRAPHPAD, La Jolla, CA, USA). $P < 0.05$ was considered statistically significant.

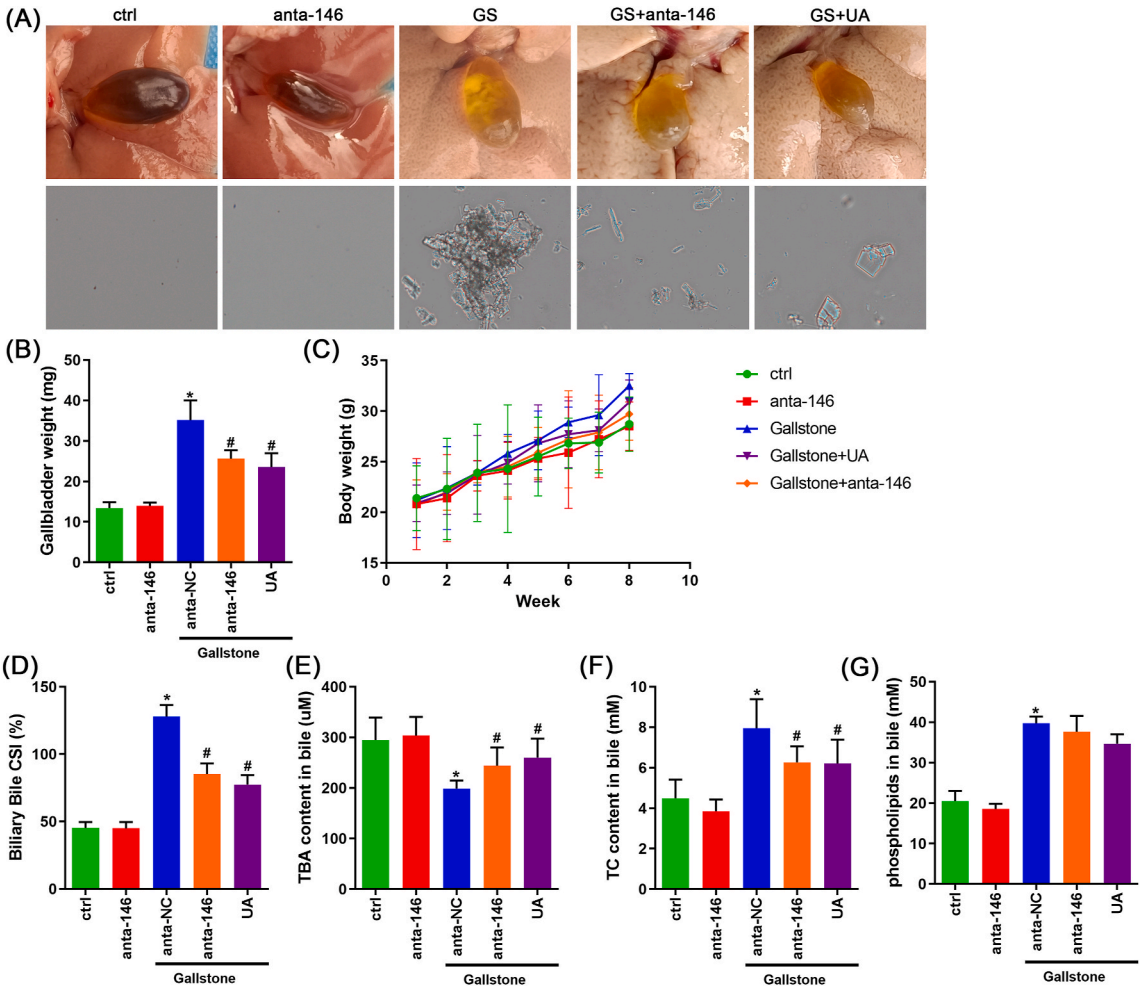

Fig. 2. The effects of anta-146 on gallstone formation in the mice fed with LD. (A) Representative images showing the gallbladders and cholesterol crystals in bile. Scale bars, 1 mm (gall bladder images) and 250 μm (cholesterol crystal images). (B) Macroscopic appearances of the gallbladders. (C) Weighted after 8 weeks of lithogenic diet treatment (n = 6 mice per group). (D) Bile lipids content and percentage. (E) total bile lipids contents. (F) The ratio of cholesterol to PL in bile. (G) CSI (n = 6–8 mice per group). Values shown are means ± SD, n = 6. *p < 0.05 vs. ctrl; #p < 0.05 vs. GS + anta-NC. UA, ursodeoxycholic acid.

3. Results

3.1. Gallbladder miR-146 level increased with LD-induced gallstone formation

To further analyze the correlation between miR-146 expression and cholesterol gallstone formation, we analyzed miR-146 level in liver and gallbladder tissues of mice fed with a lithogenic diet (Fig. 1A). miR-146 was significantly increased in gallbladder tissue compared to liver tissue (Fig. 1B). We also used qPCR and FISH probes to detect the expression and distribution of miR-146 in gallbladder samples from different groups. Compared to the control group, the GS group samples showed higher levels of miR-146, which significantly decreased after anta-146 or UA treatment (Fig. 1C and D).

3.2. Anta-miR-146 inhibited LD-induced gallstone formation

After 8 weeks of food feeding, the mice were anesthesia was executed and the gallbladder was examined. Gallstones were formed in all mice fed the lithogenic diet. In the GS group, 10 out of mice developed stones (100 %); in the anta-146 group, 3 out 10 mice developed stones (30 %). The gallbladder bile appeared dark yellow with granular stones, and microscopy revealed classic cholesterol crystals and stones (Fig. 2A). In contrast, the undaranth gallbladder bile was clear and pale yellow, with no stones or cholesterol crystals (Fig. 2A). Gallstone mass increased with LD treatment, while anta-146 and UA reduced the gallbladder weight (Fig. 2B).

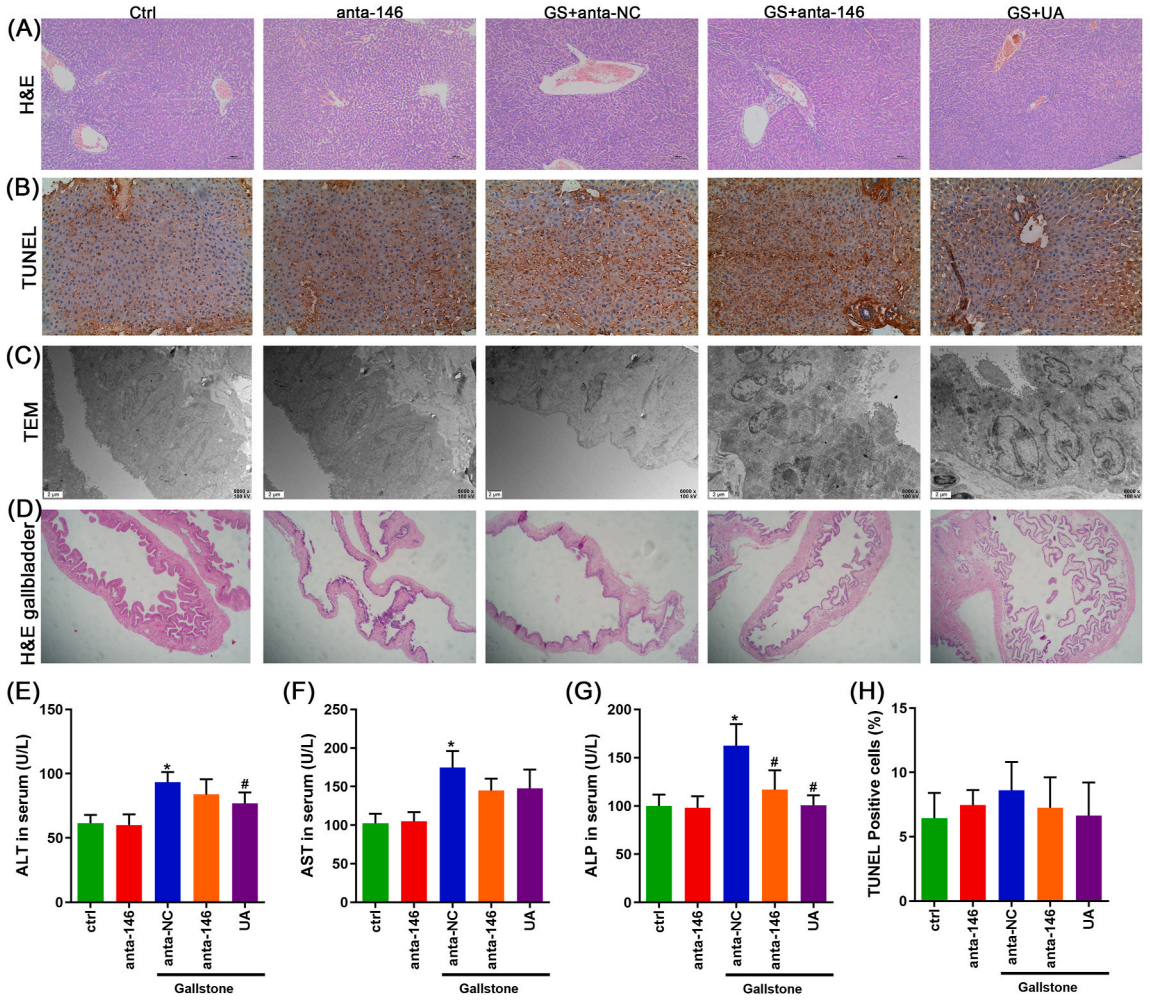

Fig. 3. The effect of miR-146a treatment on histological damages of liver or gallbladders in the mice fed with LD. (A) H&E staining and (B) TUNEL staining for liver sections. Scale bars, 100 μm. (C) Histological examination of the gallbladder by H&E staining. (D) TEM image for gallbladder sections. (E) Serum alanine aminotransferase (ALT), (F) aspartate aminotransferase (AST), and (G) alkaline phosphatase (ALP) were determined by using a Siemens fast automatic biochemical analyzer. (H) Quantification of TUNEL-positive nuclei per field in (B). Data were analyzed by ANOVA along with the post hoc Tukey test and the values shown are means ± SD, n = 6. *p < 0.05 vs. ctrl; #p < 0.05 vs. GS + anta-NC. UA, ursodeoxycholic acid.

The mice were in normal mental and physical condition, with smooth and shiny fur, and no deaths occurred during the feeding period. Weight change was calculated by subtracting the initial weight from the weight at the time of specimen collection. All four groups of mice showed weight loss. Compared to the control group, the miR-146a interference group showed a more significant decrease in body weight. Compared to the control group, the anta-146 group had a smaller decrease in body weight (Fig. 2C).

Analysis of bile flow and composition showed that miR-146 treatment did not increase bile flow in the control or GS groups, indicating no beneficial effect on bile secretion. CSI was higher in the lithogenic group than that in the control group, and reversed by anta-146 treatment (Fig. 2D). The total cholesterol in bile in the lithogenic group was higher than that of the control group, while the total bile acid content was lower than that of the control group (Fig. 2E and F). However, the bile phospholipid concentration did not change after gallstone formation (Fig. 2G).

3.3. Anta-miR-146 did not induce liver or gallbladder damage in the mice fed with LD

Changes in the structure of liver tissue and gallbladder mucosal epithelial cells were observed by H&E staining. Distinct histological features indicative of chronic biliary disease were noted in the livers of mice subjected to a low-fat diet (LD) for 8 weeks, including steatosis, spotty necrosis, hepatocyte ballooning, and lobular inflammation. Notably, compared to the GS group, the severity of hepatocellular steatosis, necrosis, and hepatocyte ballooning exhibited a significant reduction in both the anta-146 and UA groups (Fig. 3A).

TUNEL staining showed no difference in cell apoptosis among the groups. (Fig. 3B and H). TEM results showed that the gallbladder mucosal epithelial cells of mice fed with a cholesterol diet and treated with bile acids were destroyed, while the microphotographs of gallbladder mucosal histology in the model group treated with miR-146 showed that the columnar epithelial cells were opened and the cholesterol crystals were significantly reduced (Fig. 3C).

Gallbladder inflammation, characterized by thickening of the gallbladder wall, infiltration of inflammatory cells within the stromal layer, and submucosal vasodilatation, was evident in the LD group. Fewer inflammatory manifestations were observed in the anta-146 and UA groups (Fig. 3D). Serum ALT, AST, and ALP levels increased in the LD group compared to the ND group, but decreased significantly with anta-146 or UA treatments (Fig. 3E–G). These data suggested that anta-146 administration did not induce histological damage in the gallbladder and liver.

3.4. miR-146a targets megalin

Bioinformatics analysis predicted the targeting relationship between miR-146 and megalin (Fig. 4A). A dual-luciferase reporter assay in 293t cells verified that miR-146 could target and inhibit the fluorescence of megalin plasmids after transfection (Fig. 4B). Ttransfection with miR-146 mimics and inhibitors downregulated or upregulated the expression levels of megalin mRNA and protein, directly confirming megalin regulation by miR-146 (Fig. 4C–E). The mRNA level of miR-146 and megalin (Fig. 4F and G) and protein levels in the excised gallbladder tissue were detected using qPCR and immunohistochemistry. The results showed that miR-146 was negatively correlated with megalin expression levels (Fig. 4H).

3.5. Anta-miR-146 results in a change of cholesterol metabolic parameters and related genes in the mice fed with LD

Megalin could mediate cholesterol uptake from the apical surface of gallbladder epithelial cells, which was associated with cholesterol absorption and transportation in the gallbladder epithelium. Thus, we examined the effect of anta-146 on cholesterol metabolism. Following an 8-week administration of LD, mice exhibited elevated levels ofCH, LDL-C and TG, along with decreased levels of HDL-C in peripheral blood. However, treatment with anta-146 or UA resulted in a significant reduction in CH, LDL-C, and TG levels, accompanied by an increase in HDL-C levels in the serum ($^*P < 0.05$, Fig. 5A–D).

The genes CYP7A1, FXR, and SREBP-2 are key factors in the cholesterol metabolism process, including synthesis and transport. qPCR analysis indicated significant reductions in the expression levels of CYP7A1, FXR, and SREBP-2 induced by LD. The anta-146 treatment did not reverse the effect of LD on these factor expressions (Fig. 5E–G). Levels of transporter genes in liver and gallbladder tissue, involved in cholesterol efflux (ABCA1 and ABCG5/G8), cholesterol influx (SR-BI), and megalin were examined. LD significantly increased the expression of ABCG5, ABCG8, megalin and SR-BI in the gallbladder. Anta-146 did not change these gene levels except megalin (Fig. 5K). It indicates that miR-146 may not be responsible for impaired gallbladder cholesterol transport, but gallbladder cholesterol absorption via regulating megalin.

3.6. miR-146a regulate LXR-megalin/cubilin pathway related to cholesterol absorption of gallbladder

LXR is reported to regulate the expression of megalin and cubilin, which were involved in cholesterol absorption. Thus, we examined gallbladder cholesterol absorption. Utilizing radioisotope ratios in gallbladder wall tissue and gallbladder bile, our analysis revealed a decrease in cholesterol absorption and cholesterol concentrations within gallbladder wall tissues in the GS group. Notably, mice treated with anta-146 exhibited a notable enhancement in gallbladder cholesterol absorption compared to wild-type

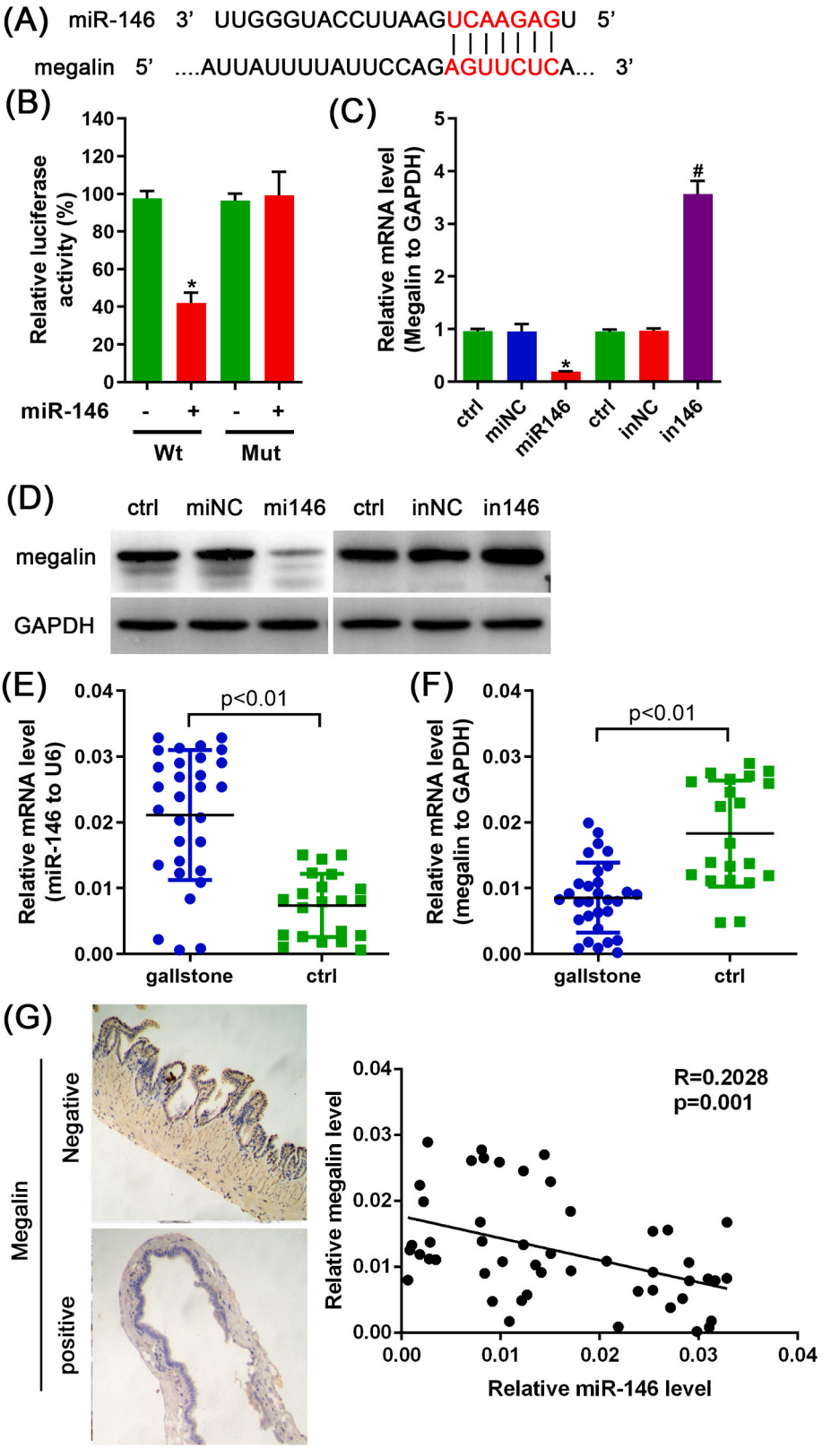

(caption on next page)

Fig. 4. miR-146 targets megalin expression. (A) Predicted binding sequences of miR-146 in 3′UTR regions of mouse megalin mRNA and (B) the effects of miR-146 mimics overexpression on luciferase activities determined from wild type or mutated forms 3′UTR reporter gene assays (n = 3 time independent experiments). (C) mRNA and (D) protein levels of megalin from 293t with miR-146 mimics or inhibitors were examined by Westen blotting (n = 3 mice per group). (E) miR-146 and (F) megalin expression levels in gallbladder were analyzed by RT-qPCR. (G) The correlation between miR-146 and megalin expression. Values shown are means ± SD, n = 6. *p < 0.05 vs. ctrl. UA, ursodeoxycholic acid.

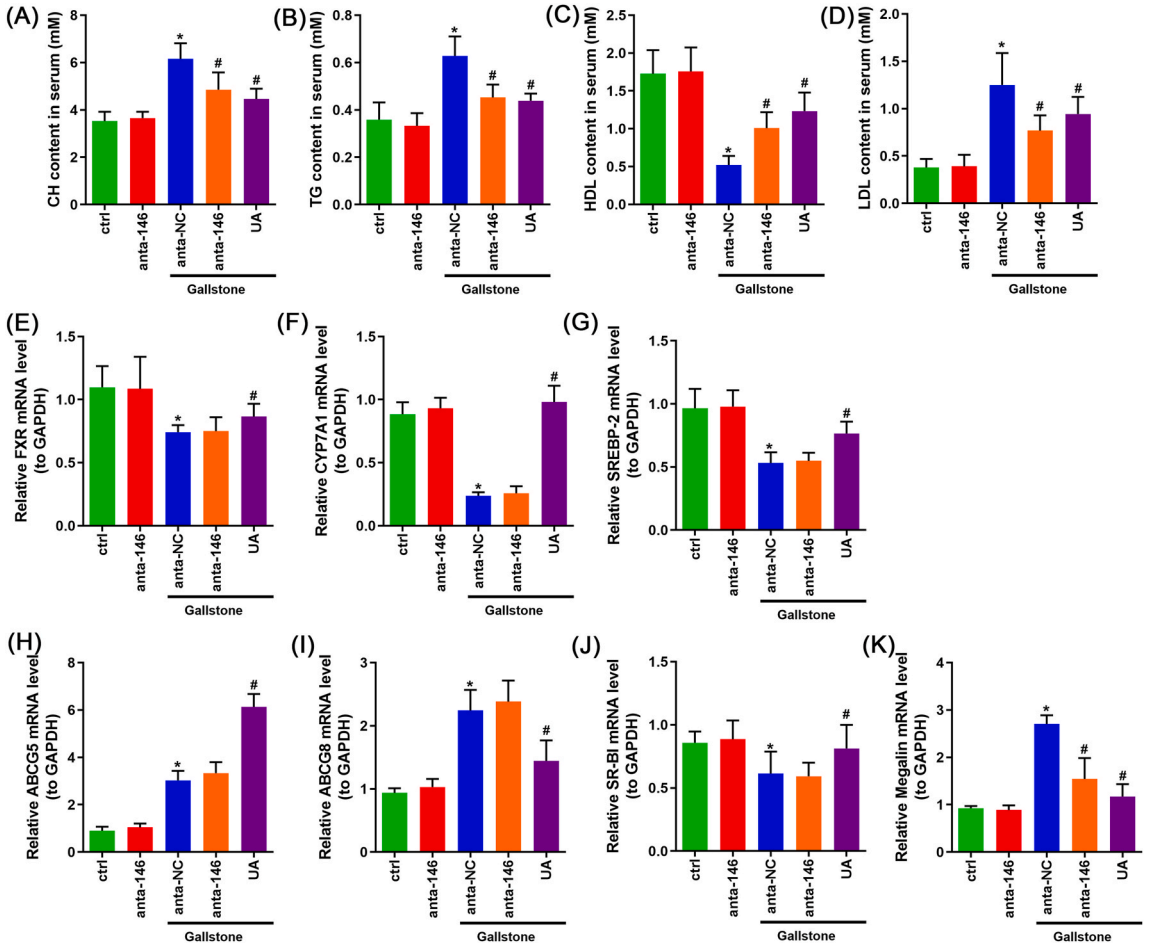

Fig. 5. The effect of miR-146a treatment on metabolic parameters and related gene expression in the mice fed with LD. The biochemistry parameters of (A) CH, (B) TG, (C) HDL-C and (D) LDL-C were separately determined in serum (n = 10 mice per group). (E) qPCR analysis of FXR, CYP7A1 and SREBP2 mRNA in liver; (F) Quantification of ABCG5, ABCG8, SR-BI and Megalin mRNA in gallbladder. Values shown are means ± SD, n = 6. *p < 0.05 vs. ctrl; #p < 0.05 vs. GS + anta-NC. UA, ursodeoxycholic acid.

counterparts, irrespective of lithogenic diet administration (Fig. 6A). Moreover, cholesterol concentrations within gallbladder wall tissues were significantly elevated in anta-146-treated mice compared to control mice (Fig. 6B).

The protein level of megalin, LXR, and cubilin expression in the excised gallbladder tissue using Western blot and immunohistochemical staining. The results showed that the protein levels of megalin, cubilin, and LXR were significantly lower in the GS group compared to the control group. The UA and anta-146a treatment groups significantly increased the expression levels of these factors (Fig. 6C and D). Consistent with the immunoblotting results, immunohistochemistry also revealed the protein expression of megalin, cubilin, and LXR in the gallbladder samples of each group (Fig. 6E–H). These data indicated that anta-146a could regulate the LXR-megalin/cubilin pathway, potentially increasing cholesterol absorption in the gallbladder.

4. Discussion

The current study demonstrated the efficacy of anta-146 treatment in preventing gallstone formation induced by LD in mice. This intervention was associated with reduced cholesterol levels, increased bile acids, and decreased CSI in bile, alongside lower levels of

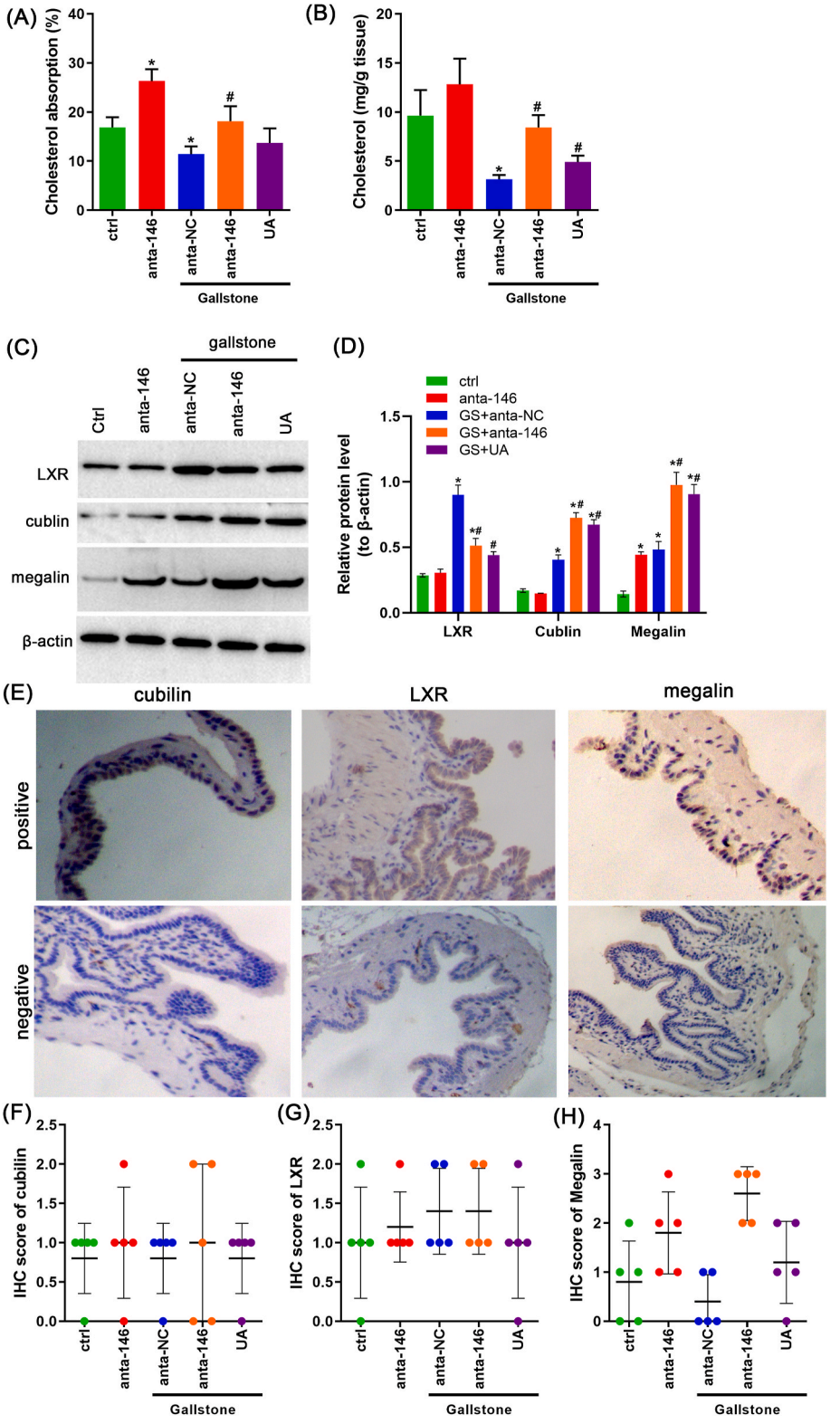

(caption on next page)

Fig. 6. The effect of miR-146a on gallbladder cholesterol absorption and regulation of LXR-megalin/cubilin expression in gallbladder from the mice fed with LD. Wild-type and GS mice (n = 6 per group) were housed individually and fed a chow diet or lithogenic diet for 4 weeks. Then anta-NC, anta-146, or UA was administrated for another 4 weeks. At 24 h after the perfusion of HDL labeled with [^{14}C] cholesterol, (A) cholesterol absorption and (B) cholesterol levels in gallbladder tissues were analyzed. (C–F) protein expression levels of LXR-megalin/cubilin in gallbladder were analyzed by Western blotting. (G) Immunohistochemistry staining for cubilin, LXR, and megalin. (H) Immunohistochemistry score of (H) cubilin, (I) LXR and (J) megalin. Values shown are means ± SD, n = 6 mice in each group. *p < 0.05 vs. ctrl; #p < 0.05 vs. GS + anta-NC. UA, ursodeoxycholic acid.

TG and CH in the systemic circulation. Anta-146 administration also ameliorated gallbladder tissue tissue damage, without impacting hepatic injury induced by LD. Subsequent analyses revealed notable upregulation of LXR-megalin expression following anta-146 treatment, while the expression of SREBP2, CYP7A1, ABCG5/8, and SR-BI in the ileum were not changed. play critical roles in cholesterol transport and absorption in the gallbladder, contributing to gallstone formation. Our primary finding underscores the pivotal role of miR-146a in modulating gallbladder cholesterol absorption and the formation of cholesterol gallstones by targeting key cholesterol absorption, particularly megalin.

We first observed a notable elevation in miR-146a expression within the mouse gallbladder rather than in liver in response to LD supplemented with 1.25 % cholesterol. Given the comparatively lower abundance of miR-146 within hepatocytes, we suggest that alterations in liver miR-146 expression may not accurately reflect the underlying conditions affecting hepatocytes. Subsequently, we confirmed the inhibitory effect of anta-146 on the formation of gallstones. Increasingly, studies have identified varous miRNAs involved in gallstones formation, such as circulating miR-122 [28], miR-210 [29], miR-29a [30], and other miRNAs correlating with gallstones incidence. For instance, miR-223 regulates the bile cholesterol secretion in liver by targeting ABCG5 and ABCG8, thereby inhibiting gallstone formation in mice [21]. These results suggest that the therapeutic potential of miRNAs in gallstones formation.

Using bioinformatics, we identified megalin as a target of miR-146a. Megalin is an important cholesterol transport protein that plays a key role in regulating cholesterol transport [31]. In Liang et al.'s study [32], the single-cell RNA sequencing data revealed reduced expression levels of transporter genes, particularly apical membrane transporters such as Npc1l1, ABCG5, and ABCG8. This observation suggests that gallbladder epithelial cells may exhibit limited activity in both cholesterol absorption from bile and its excretion into bile, thereby constraining their ability to regulate cholesterol content within bile during lithogenesis. Notably, megalin, in conjunction with cubilin, facilitates the endocytosis of various ligands, including HDL/apolipoprotein A-I (APOA-1), which are implicated in cholesterol absorption by the gallbladder epithelium [33].

To further explore the role of miR-146 in cholesterol gallstone formation, we assessed its effect involved in cholesterol biosynthesis, uptake, and efflux. Our results showed that miR-146 did not affect these functions. Following anta-146 treatment, we observed increased megalin/cubilin levels in gallbladder tissue. However, we did not detect increased expression of ABCG5 and ABCG8 in the gallbladder tissue, which contributes to cholesterol levels in bile secreted by the liver and stored in the gallbladder. Similarly, there was no discernible augmentation in SR-BI protein expression, an ABCG5/8-independent cholesterol transporter predominantly found in canalicular membranes, responsible for facilitating biliary cholesterol secretion under normal physiological conditions [34]. Nevertheless, anta-146 affected the expression of LXR-megalin in gallbladder tissue. Our data suggests that miR-146a likely targets the reactivation of apical membrane transporters—megalin, which regulates cholesterol absorption in gallbladder tissue.

Normal gallbladder epithelium plays a crucial role in maintaining bile composition, thus preventing cholesterol supersaturation [4]. However, this ability is impaired in in patients with cholesterol gallstones. Corradini et al. [13] developed a direct methodological approach using an ex vivo isolated gallbladder model with negative internal perfusion to elucidate the impact of gallbladder epithelium on bile. Their results showed a significantly reduced cholesterol absorption rate in patients with cholesterol gallstones compared to the control group, alongside a lower bile salt absorption rate. Thus, gallstones lead to more lithogenic bile, resulting in a significant increase in cholesterol and a decrease in the molar percentage of bile salts due to impaired lipid absorption [35]. Consistent with previous findings, we observed that anta-146-treated mice exhibited significant increases gallbladder cholesterol absorption and cholesterol levels in the gallbladder wall tissue than wild-type mice. Combined with the excessive secretion of liver-bile cholesterol, this defect in cholesterol absorption represents another facilitating factor in cholesterol gallstones formation [35].

This study validated the role of miR-146a on gallstone formation in vivo and suggested that it may regulate LXR/megalin/cubilin pathway involved in cholesterol absorption. While this study was limited to in vivo experiments, further research should evaluate the protein levels of cholesterol-related genes in vitro to confirm these conclusions. Given that miRNAs can regulate many target genes, other genes maybe also infuluence gallstone formation. More fundamental experiments are warranted to elucidate the specific physiological mechanisms by which miR-146 affects cholesterol absorption-related genes, assessing the therapeutic potential of gene agonists applicable to gallstones.

5. Conclusions

In summary, this study highlights the preventive role of anta-146 against LD-induced gallstone formation and the restoration of cholesterol homeostasis. These effects are attributed to the modulation of LXR-megalin-cubilin expression, which regulates gallbladder cholesterol absorption. Our findings imply that the miR-146/megalin axis may facilitate gallbladder cholesterol absorption and prevent cholesterol gallstones formation.

Availability of data and materials

All data generated or analyzed during this study are included in the article.

Ethics approval

This study was performed in line with the principles of the Declaration of Helsinki. Approval was granted by the Ethics Committee of the First Affiliated Hospital of Kunming Medical University (No.2020-031). Informed consent was obtained from all individual participants included in the study.

All animals used in this study were treated strictly according to the National Institutes of Health Guidelines for the Care and Use of Laboratory Animals. All procedures were approved by the Animal Care Review Committee, Kunming Medical University, China.

Financial support and sponsorship

This work was supported by the National Natural Science Foundation of China (81860121); Yunnan Applied Basic Research Projects-Kunming Medical University Union Foundation (202001AY070001-040); Yunnan Provincial Fund for High Level Reserve Talents in Health Science (H-2018068).

CRediT authorship contribution statement

Bin Yang: Writing – review & editing, Writing – original draft, Data curation, Conceptualization. **Pingli Cao:** Methodology, Investigation, Formal analysis. **Guoqing Bao:** Software, Resources, Methodology, Investigation. **Ming Wu:** Validation, Software, Resources. **Weihong Chen:** Validation, Software, Resources, Investigation. **Shuangyan Wu:** Validation, Software, Investigation, Formal analysis. **Ding Luo:** Writing – review & editing, Funding acquisition, Conceptualization. **Pinduan Bi:** Writing – review & editing, Writing – original draft, Data curation, Conceptualization.

Declaration of competing interest

The authors declare that they have no known competing financial interests or personal relationships that could have appeared to influence the work reported in this paper.

Acknowledgments

This work was supported by the National Natural Science Foundation of China (81860121); Yunnan Applied Basic Research Projects-Kunming Medical University Union Foundation (202001AY070001-040); Yunnan Provincial Fund for High Level Reserve Talents in Health Science (H-2018068).

Appendix A. Supplementary data

Supplementary data to this article can be found online at https://doi.org/10.1016/j.heliyon.2024.e36679.

References

[1] B.J. Finch, P.D. Robinson, C.H. Wakefield, What you need to know about gallstone disease, Br. J. Hosp. Med. 83 (12) (2022) 1–8.
[2] C. Gutt, S. Schläfer, F. Lammert, The treatment of gallstone disease, Deutsches Ärzteblatt International 117 (9) (2020) 148.
[3] S. Haal, et al., Risk factors for symptomatic gallstone disease and gallstone formation after bariatric surgery, Obes. Surg. 32 (4) (2022) 1270–1278.
[4] H. Sun, et al., Factors influencing gallstone formation: a review of the literature, Biomolecules 12 (4) (2022) 550.
[5] A.R. Dosch, D.K. Imagawa, Z. Jutric, Bile metabolism and lithogenesis: an update, Surgical Clinics 99 (2) (2019) 215–229.
[6] D. Kiran, S. Rani, S. Swain, Lithogenic modulator mechanisms: current and future directions, J. Pharmaceut. Sci. Res. 14 (7) (2022) 795–800.
[7] H.H. Wang, et al., Effects of biliary phospholipids on cholesterol crystallization and growth in gallstone formation, Adv. Ther. (2023) 1–26.
[8] R.V. Rege, Inflammatory cytokines alter human gallbladder epithelial cell absorption/secretion, J. Gastrointest. Surg. 4 (2) (2000) 185–192.
[9] Y.B. Dayan, A. Vilkin, Y. Niv, Gallbladder mucin plays a role in gallstone formation, Eur. J. Intern. Med. 15 (7) (2004) 411–414.
[10] J. Miquel, et al., Expression and regulation of scavenger receptor class B type I (SR-BI) in gall bladder epithelium, Gut 52 (7) (2003) 1017–1024.
[11] Z.-Y. Jiang, et al., Increased expression of LXRα, ABCG5, ABCG8, and SR-BI in the liver from normolipidemic, nonobese Chinese gallstone patients, J. Lipid Res. 49 (2) (2008) 464–472.
[12] Y. Chen, J. Kong, S. Wu, Cholesterol gallstone disease: focusing on the role of gallbladder, Lab. Invest. 95 (2) (2015) 124–131.
[13] S.G. Corradini, et al., Impaired human gallbladder lipid absorption in cholesterol gallstone disease and its effect on cholesterol solubility in bile, Gastroenterology 118 (5) (2000) 912–920.
[14] T.X. Lu, M.E. Rothenberg, MicroRNA, J. Allergy Clin. Immunol. 141 (4) (2018) 1202–1207.
[15] G. Michlewski, J.F. Cáceres, Post-transcriptional control of miRNA biogenesis, Rna 25 (1) (2019) 1–16.
[16] W. Kim, E. Kyung Lee, Post-transcriptional regulation in metabolic diseases, RNA Biol. 9 (6) (2012) 772–780.
[17] A. Bhattarai, et al., Regulation of cholesterol biosynthesis and lipid metabolism: a microRNA management perspective, Steroids 173 (2021) 108878.
[18] K.M. Citrin, C. Fernández-Hernando, Y. Suárez, MicroRNA regulation of cholesterol metabolism, Ann. N. Y. Acad. Sci. 1495 (1) (2021) 55–77.

[19] Q. Liu, et al., Polyunsaturated fatty acids ameliorate renal stone-induced renal tubular damage via miR-93-5p/Pknox1 axis, Nutrition 105 (2023) 111863.
[20] L. Huang, et al., Integrated analysis of mRNA-seq and miRNA-seq reveals the potential roles of Egr1, Rxra and Max in kidney stone disease, Urolithiasis 51 (1) (2022) 13.
[21] F. Zhao, et al., miRNA-223 suppresses mouse gallstone formation by targeting key transporters in hepatobiliary cholesterol secretion pathway, Int. J. Biol. Sci. 17 (15) (2021) 4459.
[22] B. Yang, et al., An integrated analysis of differential miRNA and mRNA expressions in human gallstones, Mol. Biosyst. 11 (4) (2015) 1004–1011.
[23] K. Li, et al., miR-146a improves hepatic lipid and glucose metabolism by targeting MED1, Int. J. Mol. Med. 45 (2) (2020) 543–555.
[24] L.J. Chen, et al., MicroRNA-146a deficiency promotes atherosclerosis by dysregulating cholesterol homeostasis in macrophages, Faseb. J. 32 (2018), 752.6-752.6.
[25] K. Matsumoto, et al., Claudin 2 deficiency reduces bile flow and increases susceptibility to cholesterol gallstone disease in mice, Gastroenterology 147 (5) (2014) 1134–1145. e10.
[26] H.H. Wang, et al., Evidence that gallbladder epithelial mucin enhances cholesterol cholelithogenesis in MUC1 transgenic mice, Gastroenterology 131 (1) (2006) 210–222.
[27] M.W. Pfaffl, Relative quantification, in: Real-time PCR, Taylor & Francis, 2007, pp. 89–108.
[28] F. Th'ng, et al., Evaluation of plasma microRNA-122, high-mobility group box 1 and keratin-18 concentrations to stratify acute gallstone disease: a pilot observational cohort study in an emergency general surgery unit, BMJ Open 8 (4) (2018) e020061.
[29] F.C.S. Th'Ng, Role of microRNA Biomarkers to Predict Complications of Gallstones, 2015.
[30] J. Li, et al., Roles of microRNA-29a in the antifibrotic effect of farnesoid X receptor in hepatic stellate cells, Mol. Pharmacol. 80 (1) (2011) 191–200.
[31] G.F. Lewis, D.J. Rader, New insights into the regulation of HDL metabolism and reverse cholesterol transport, Circ. Res. 96 (12) (2005) 1221–1232.
[32] J. Liang, et al., Single cell RNA-sequencing reveals a murine gallbladder cell transcriptome atlas during the process of cholesterol gallstone formation, Front. Cell Dev. Biol. 9 (2021) 714271.
[33] A.K. Tsaroucha, et al., Megalin and cubilin in the human gallbladder epithelium, Clin. Exp. Med. 8 (2008) 165–170.
[34] K.S. Bura, et al., Intestinal SR-BI does not impact cholesterol absorption or transintestinal cholesterol efflux in mice, J. Lipid Res. 54 (6) (2013) 1567–1577.
[35] H.H. Wang, P. Portincasa, D.Q.-H. Wang, Molecular pathophysiology and physical chemistry of cholesterol gallstones, Frontiers in Bioscience-Landmark 13 (2) (2008) 401–423.